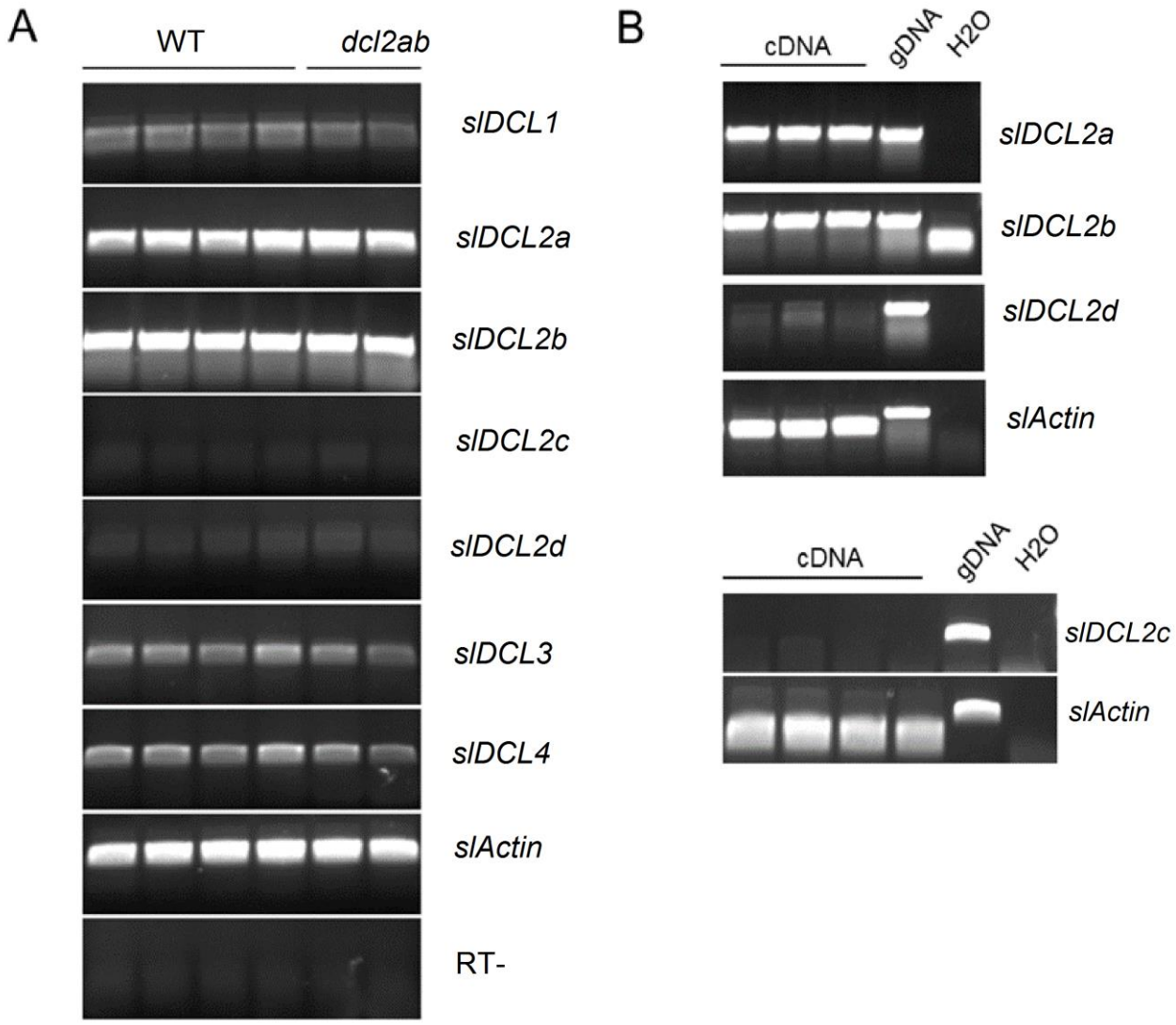

Supplemental Figure S1. (**A**) RT-PCR of *slDCL*s in M82 and the *dcl2ab* mutant. Total RNA was extracted from 24-day-old leaves and then cDNA was synthesized with oligodT primer. PCR products of 28 cycles were segregated in 1.5% agarose gel. Genomic DNA and H_2O as positive and negative controls, respectively. (**B**) PCR of *slDCL2s* in M82 cDNA and genomic DNA (gDNA). PCR products were obtained from gDNA, suggesting that lack of PCR products from cDNA is due to lower gene expression instead of failure of PCR.

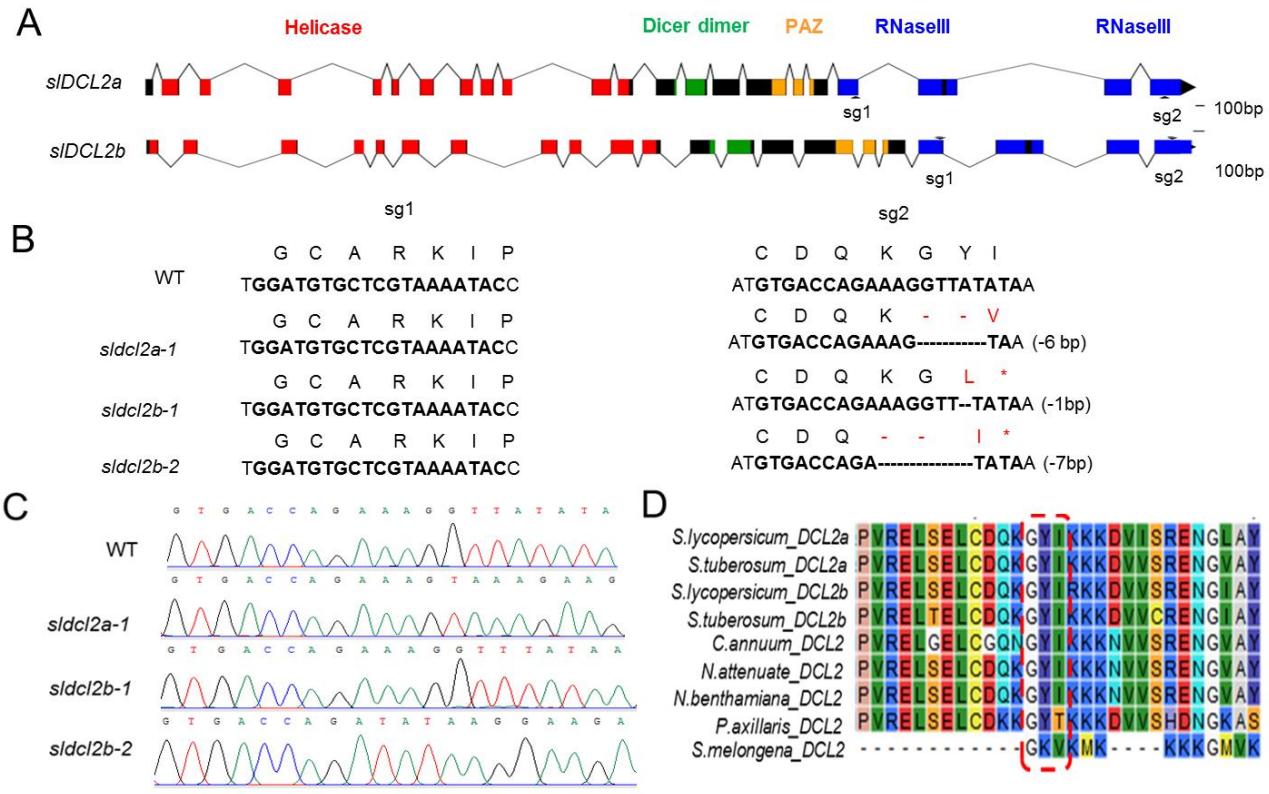

Supplemental Figure S2. *slDCL2* mutants. (**A**) Gene structures of slDCL2a and slDCL2b. Exons and introns are indicated by rectangles and lines respectively. Functional domains are labelled with different colours. Small guide RNA (sgRNA) targets are marked with arrowheads; (**B**) Encoded amino acids of sgRNA target regions are shown. Amino acid changes by mutation are highlighted in red; (**C**) Sanger sequencing results of mutations; (**D**) Protein sequence alignments of DCL2 in *Solanaceae*. The mutation region is marked by red rectangle.

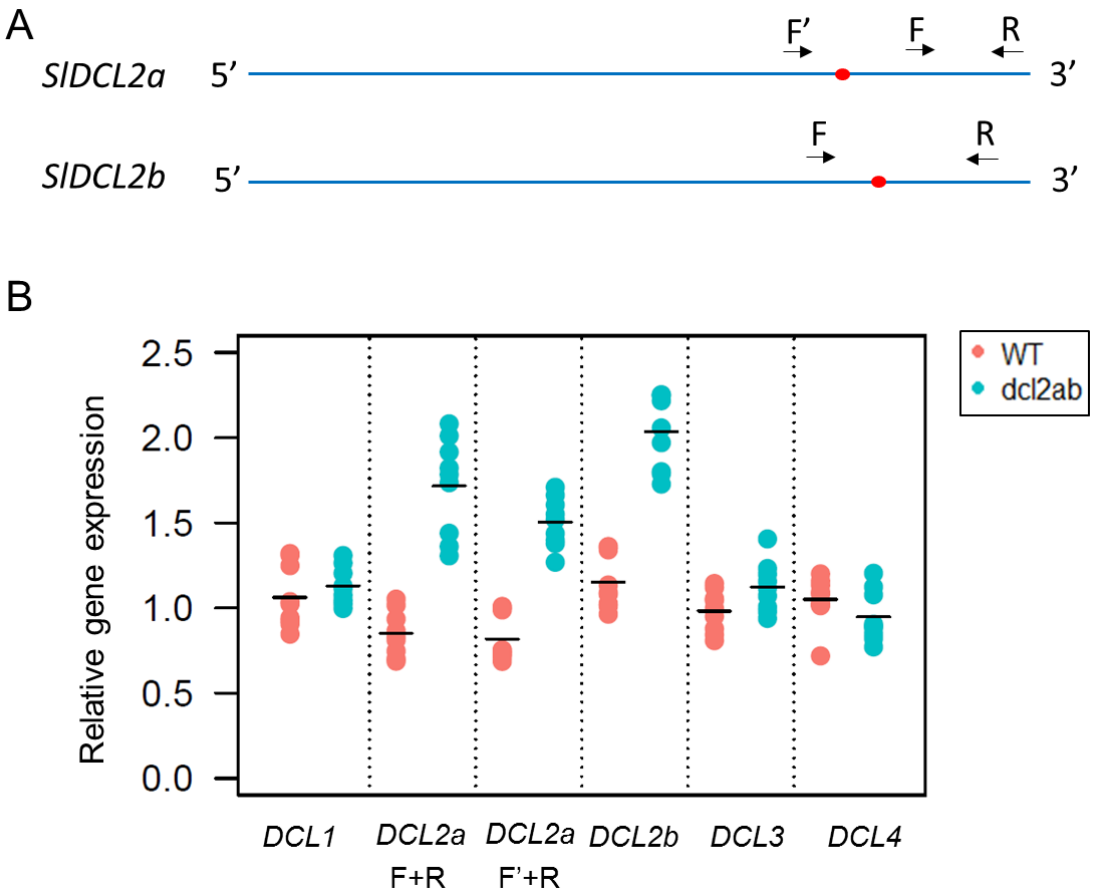

Supplemental Figure S3. (**A**) Schemes of RT-PCR primers of *SlDCL2a* and *SlDCL2b*. Dark blue lines represent mRNAs. Red dots indicate the mutations. Forward and reverse primers are marked with F or F' and R arrowheads; (**B**) RT-qPCR of *slDCL*s in WT and the *dcl2ab* mutant. *slActin7* was used as endogenous control.

Supplemental Figure S4. Phenotypes of *dcl2a*, *dcl2b* and *dcl2ab*.

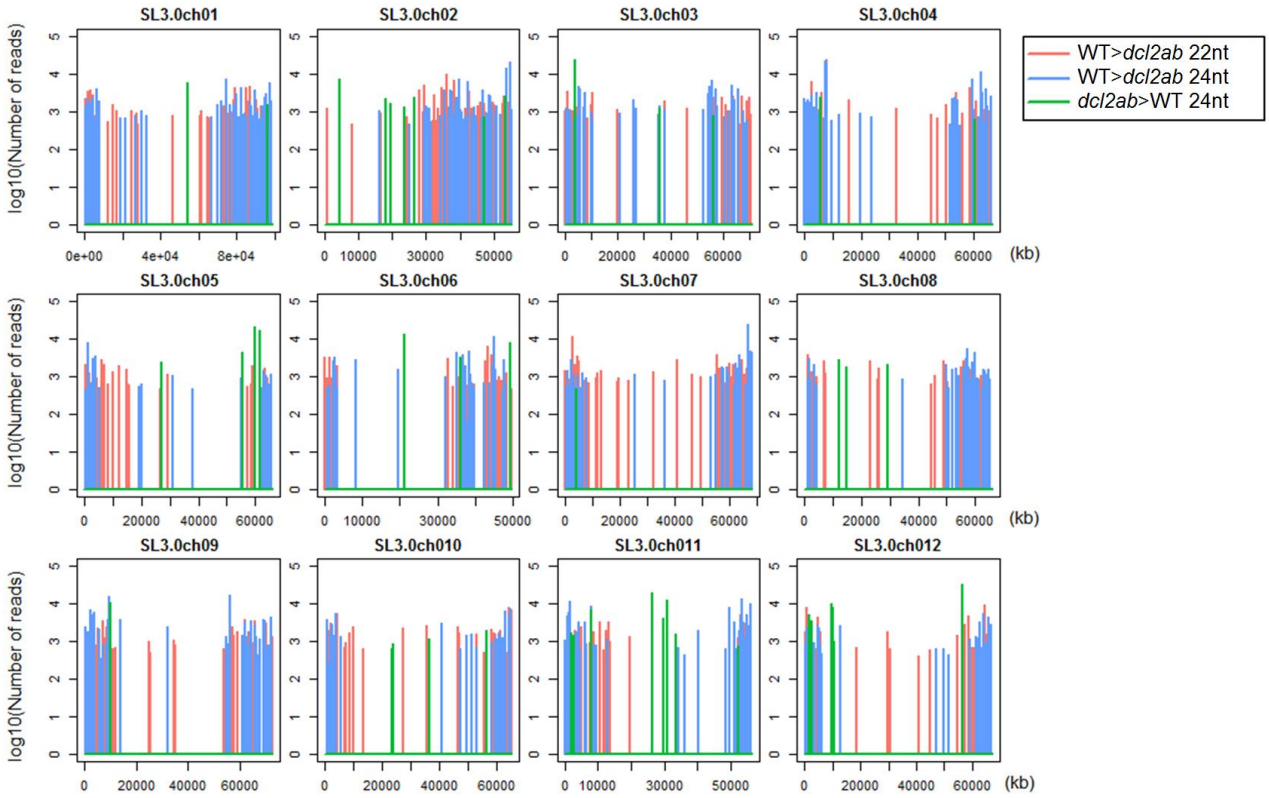

Supplemental Figure S5. Chromosomal distribution of DE loci in WT and *dcl2ab*. X-axis shows the chromosomal coordinates, and y-axis shows the log10 values of sRNA reads in WT for 22nt and 24nt D2 loci and in *dcl2ab* for 24nt D2i loci.

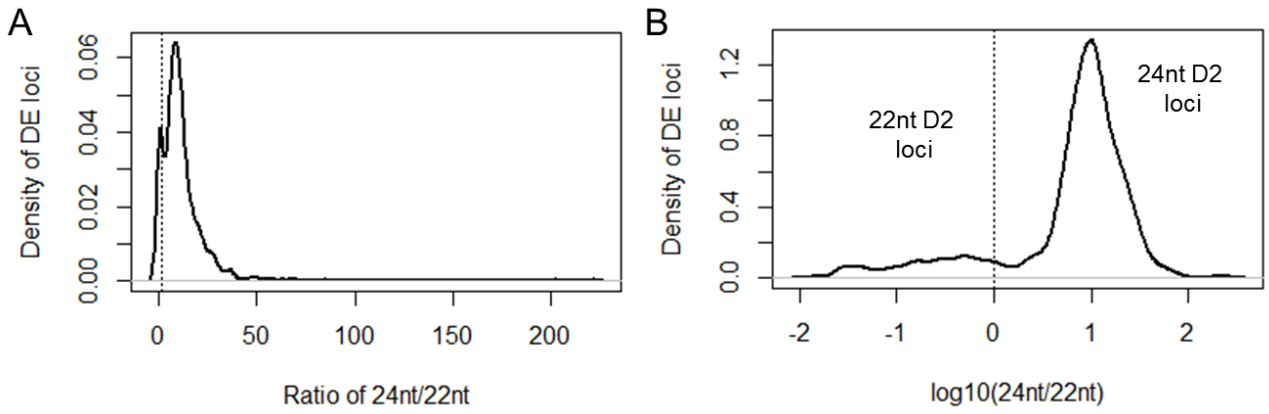

Supplemental Figure S6. Ratio of 24nt/22nt sRNA loci of the tomato genome. The sRNA were analysed for differential expression (DE) loci between WT and *dcl2ab* by segmentSeq (Hardcastle 2010). There are 1, 215 DE loci including 647 ones that are downregulated in *dcl2ab* than WT (D2 loci) and 568 that were upregulated in *dcl2ab* (D2i loci). Kernel density plots show the density of D2 loci vs the ratio of 24nt sRNA: 22nt sRNA within each locus **(A)** or the log10 value of ratio **(B)**. Vertical lines indicate 24nt:22nt=1 so that loci on the left are 22nt predominant D2 loci and those on the right are 24nt predominant D2 loci.

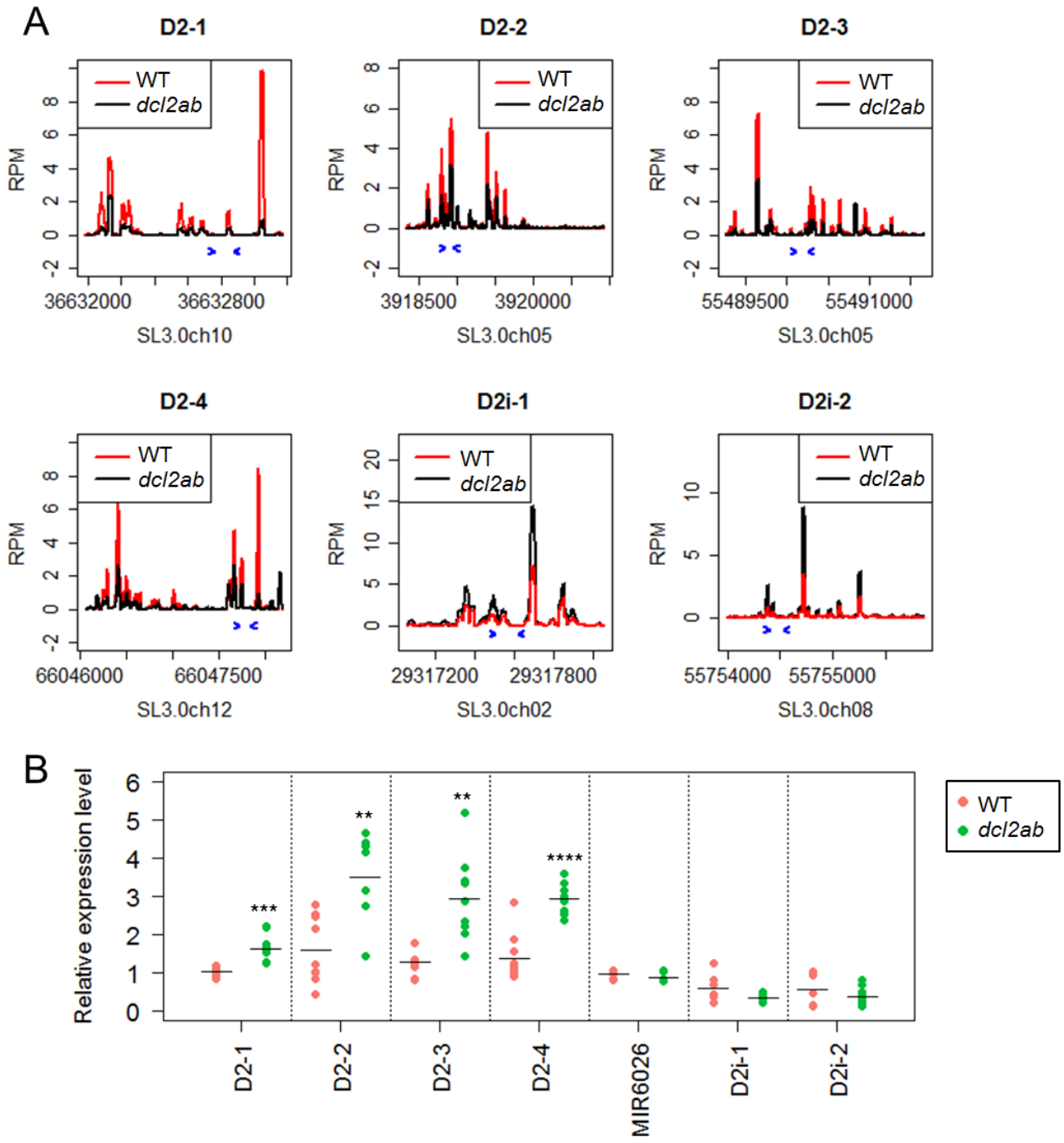

Supplemental Figure S7. A. sRNA RPM plots showing accumulation of sRNAs mapped to five D2 and two D2i loci in WT and *dcl2ab*. Primers used in **B** are marked with arrowheads; **B.** RT-qPCR results of D2 and D2i precursors, including pre-miR6026, in WT and *dcl2ab*. *slActin* was used as control. ** $p < 0.01$, *** $p < 0.001$, **** $p < 0.0001$.

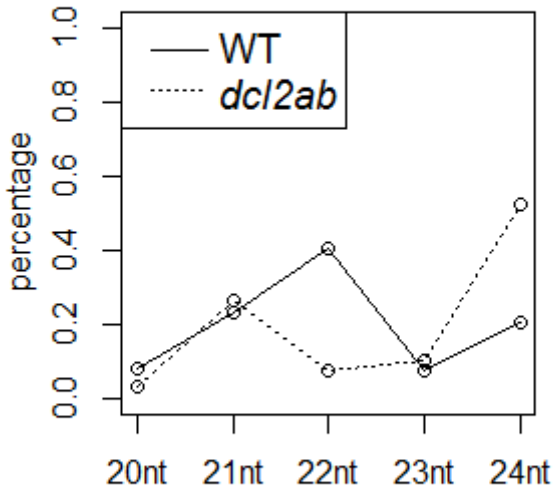

Supplemental Figure S8. 24-nt D2i sRNA regions produce more 22-nt sRNAs in WT than *dcl2ab*. 24-nt D2i sRNA sequences were collected and used as Bowtie alignment reference of WT and *dcl2ab* sRNA sequencing data. Percentage shows the composition of different sizes of sRNAs from the 24-nt D2i sRNA regions in WT and *dcl2ab*.

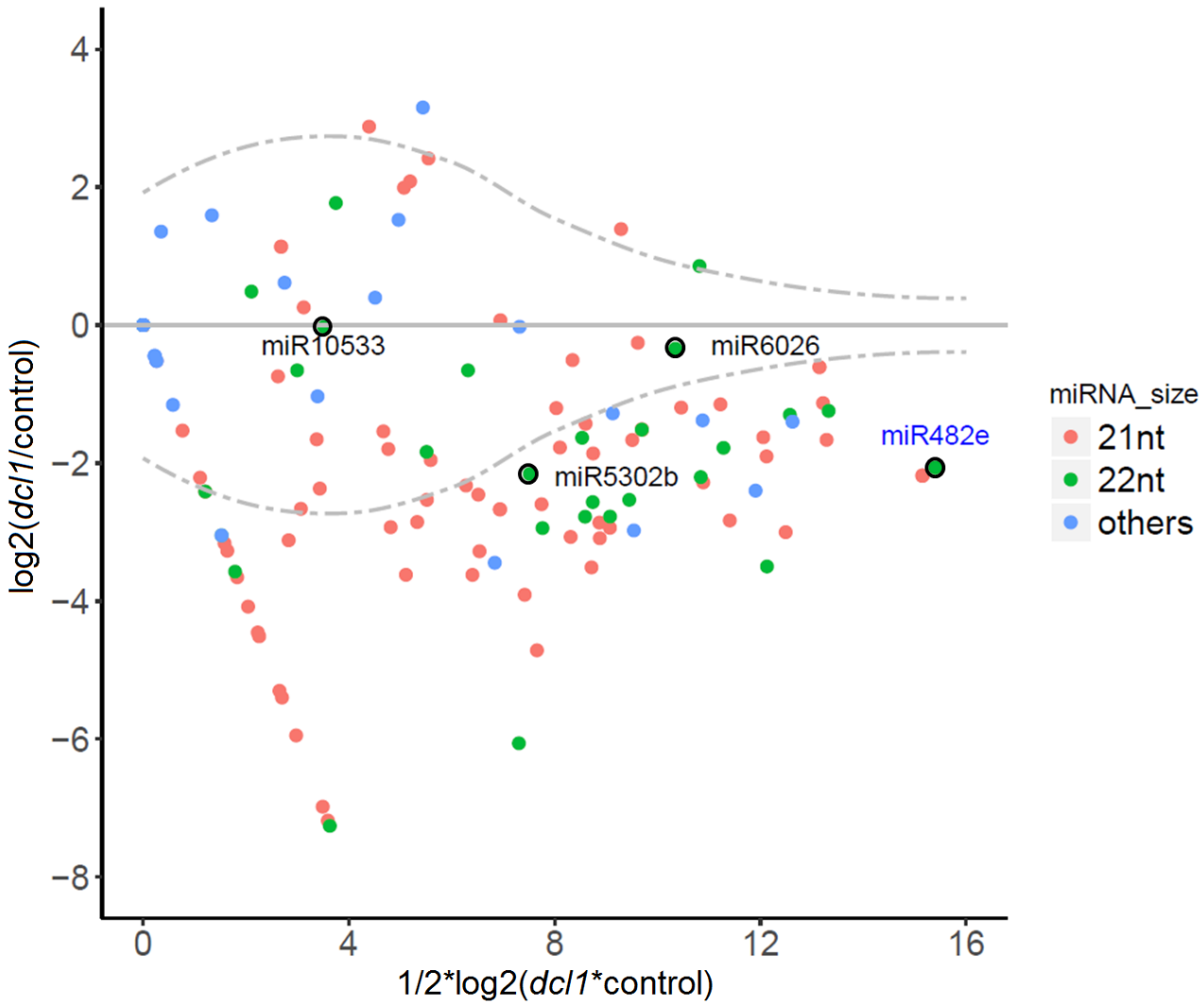

Supplemental Figure S9. MA Plot showing miRNA abundance in WT and *dcl1* by re-analyzing published *dcl1* sRNA-seq data (Kravchik et al. 2014). 21-nt and 22-nt sizes of miRNAs are shown in different colours. Three slDCL2-dependent miRNAs (miR6026, miR5302b and miR10533) and one slDCL1-dependent miRNA (miR482e) are marked.

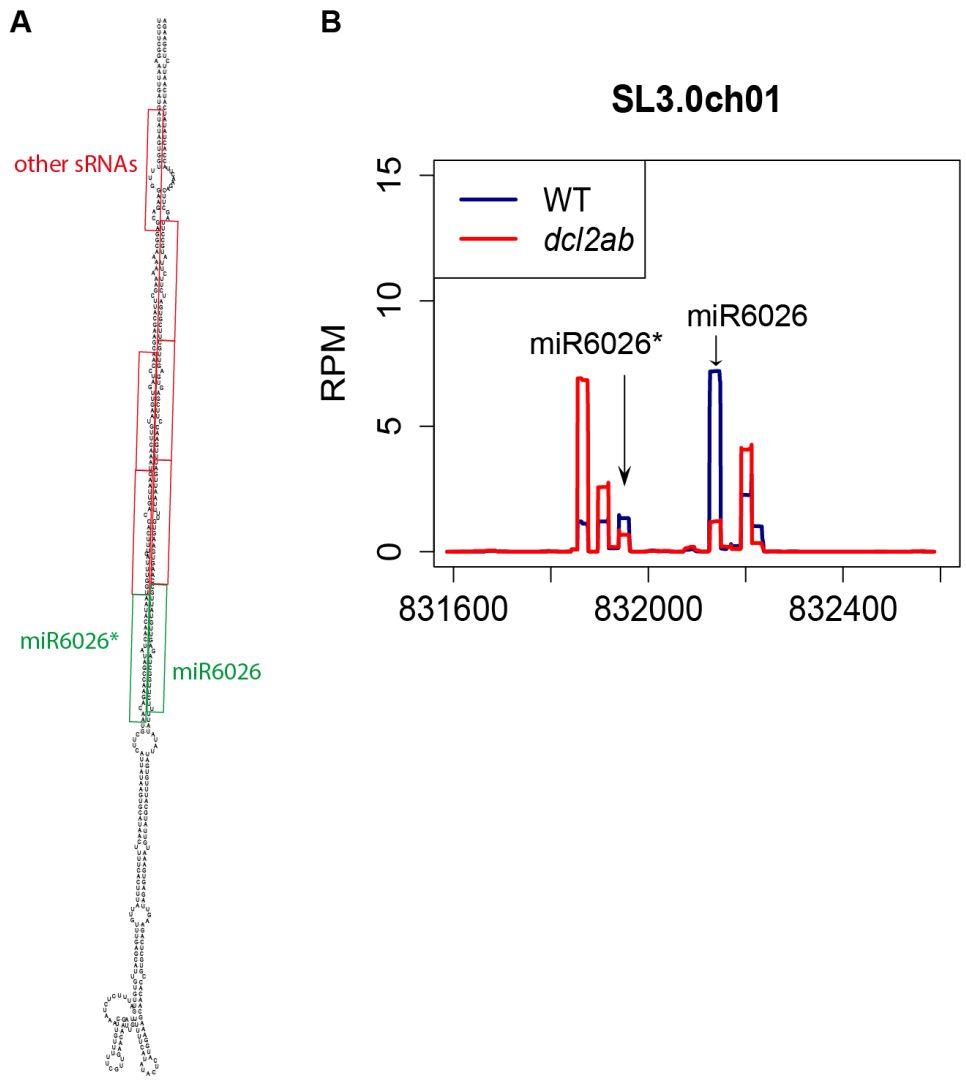

Supplemental Figure S10. A. Stem loop structure of miR6026 precursor. miR6026/miR6026* and other sRNAs are marked in green and red, respectively. **B.** sRNA RPM plots showing accumulations of sRNAs from pre-miR6026 in WT and *dcl2ab*. Mature miR6026 and miR6026* are marked with arrowheads.

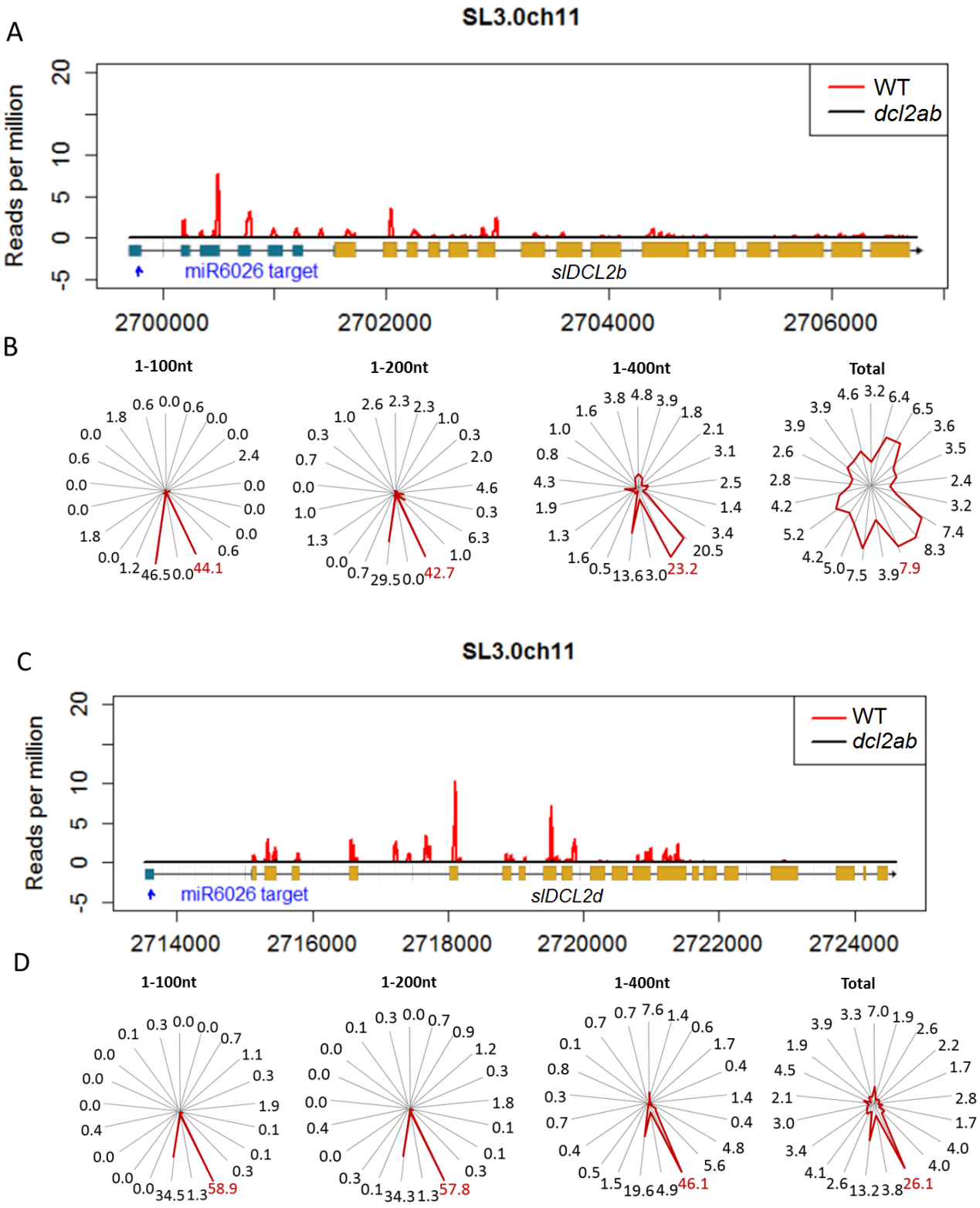
A
SL3.0ch11
Reads per million
20
10
5
0
-5
WT
dcl2ab
miR6026 target
slDCL2b
2700000
2702000
2704000
2706000
B
1-100nt
0.6 0.0 0.6 1.8 0.0 0.0 0.0 2.4 0.6 0.0 0.0 0.0 0.0 1.8 0.0 0.6 1.2 46.5 0.0 44.1
1-200nt
2.6 2.3 2.3 1.0 1.0 0.3 0.3 2.0 0.7 0.0 4.6 1.0 0.3 6.3 1.3 0.0 1.0 0.7 29.5 0.0 42.7
1-400nt
3.8 4.8 3.9 1.6 1.8 1.0 2.1 0.8 3.1 4.3 2.5 1.9 1.4 1.3 3.4 1.6 20.5 0.5 13.6 3.0 23.2
Total
4.6 3.2 6.4 3.9 6.5 3.9 3.6 2.6 3.5 2.8 2.4 4.2 3.2 5.2 7.4 4.2 8.3 5.0 7.5 3.9 7.9
C
SL3.0ch11
Reads per million
20
10
5
0
-5
WT
dcl2ab
miR6026 target
slDCL2d
2714000
2716000
2718000
2720000
2722000
2724000
D
1-100nt
0.1 0.3 0.0 0.0 0.7 0.0 1.1 0.0 0.3 0.0 1.9 0.4 0.1 0.0 0.1 0.0 0.3 0.0 0.0 34.5 1.3 58.9
1-200nt
0.1 0.3 0.0 0.7 0.9 0.0 1.2 0.0 0.3 0.0 1.8 0.4 0.1 0.0 0.1 0.3 0.1 34.3 1.3 57.8
1-400nt
0.7 0.7 7.6 1.4 0.6 0.1 1.7 0.8 0.4 0.3 1.4 0.7 0.4 0.4 4.8 0.5 5.6 1.5 19.6 4.9 46.1
Total
3.9 3.3 7.0 1.9 2.6 1.9 2.2 4.5 1.7 2.1 2.8 3.0 1.7 3.4 4.0 4.1 4.0 2.6 13.2 3.8 26.1

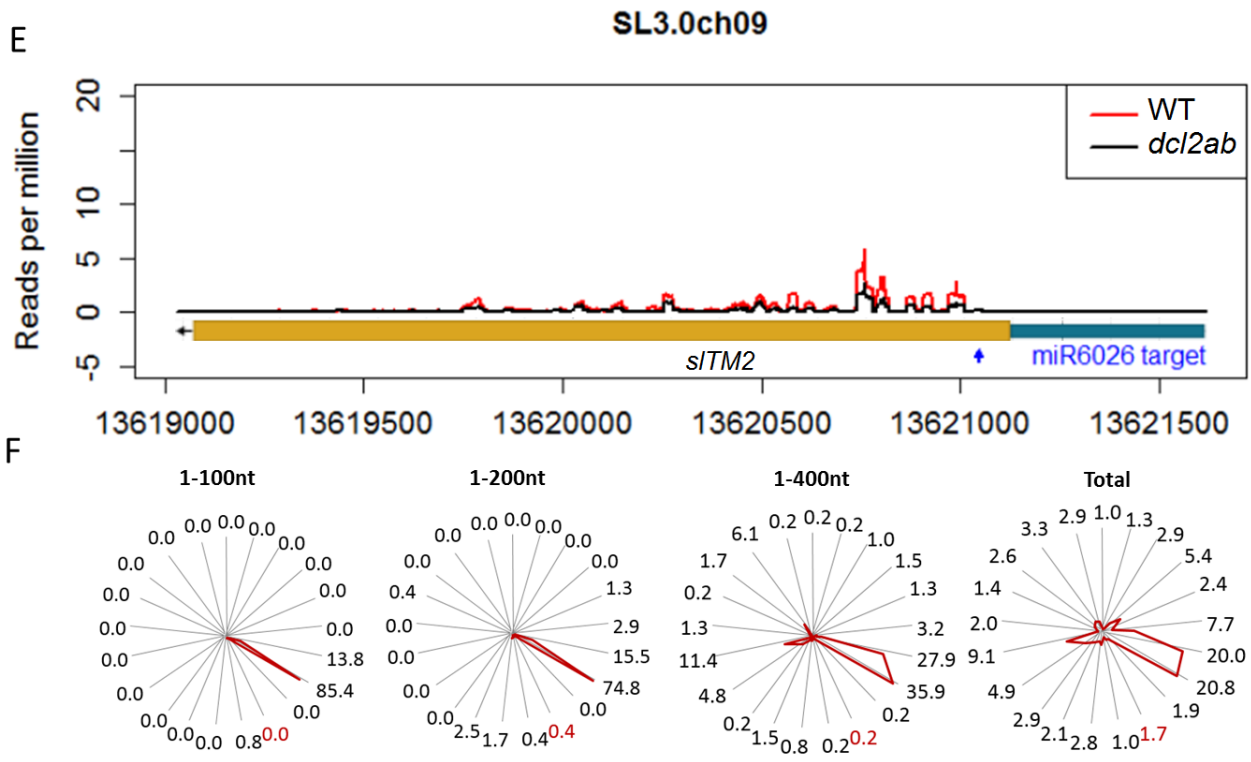

Supplemental Figure S11. Accumulation of *slDCL2b* and *slDCL2d* sRNA, not *slTM2* sRNA, is reduced in *dcl2ab*. (**A, C, E**) sRNA RPM plots showing the levels of *slDCL2a*, *slDCL2d*, and *slTM2* sRNAs in WT and *dcl2ab*. The p-values of *slDCL2a*, *slDCL2b*, *slDCL2d* and *slTM2* sRNA between WT and *dcl2ab* are 0.01, 0.0008, 0.003 and 0.11, respectively. In the gene models, rectangles and lines represent exons and introns, respectively. UTRs and ORFs are in cyan and yellow, respectively. Arrows mark the direction of transcription. Target site of miR6026 is marked with blue arrowhead; (**B, D, F**) The phasing of *slDCL2a*, *slDCL2d* and *slTM2* sRNAs in WT. Radar plots show percentages of 21-nt reads corresponding to each of the 21 registers from the whole transcript of *slDCL2b*, or 1-100nt, 1-200nt, 1-400nt of the *slDCL2b* transcript in WT sRNA-seq data. The 10th position (in red) indicates the miR6026-guided cleavage site between the 10th and 11th nucleotide of miR6026.

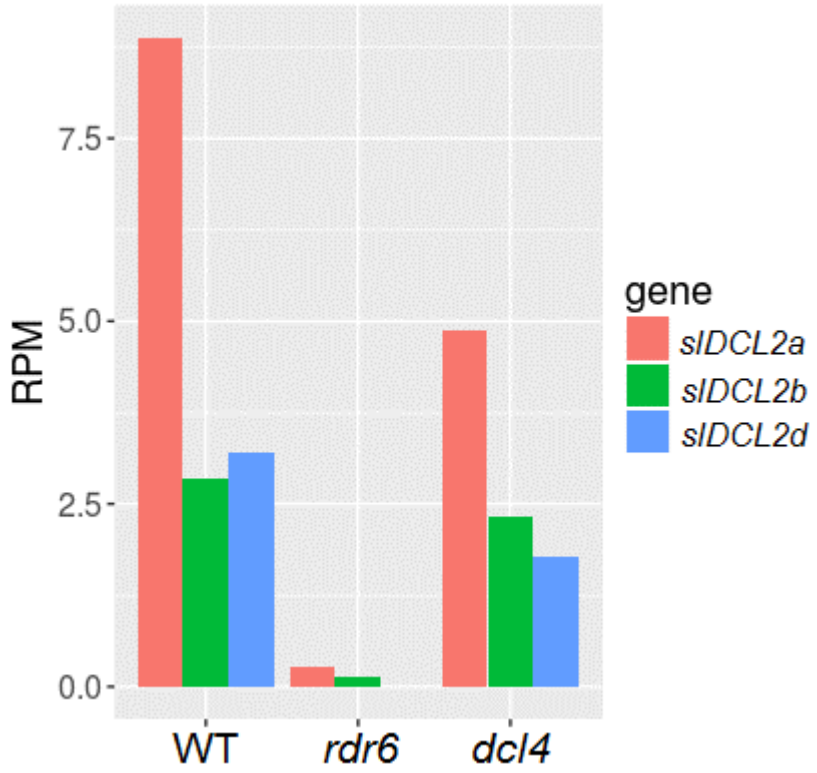

Supplemental Figure S12. RPM plot of *SlDCL2* sRNA in WT, *rdr6*, and *dcl4*.

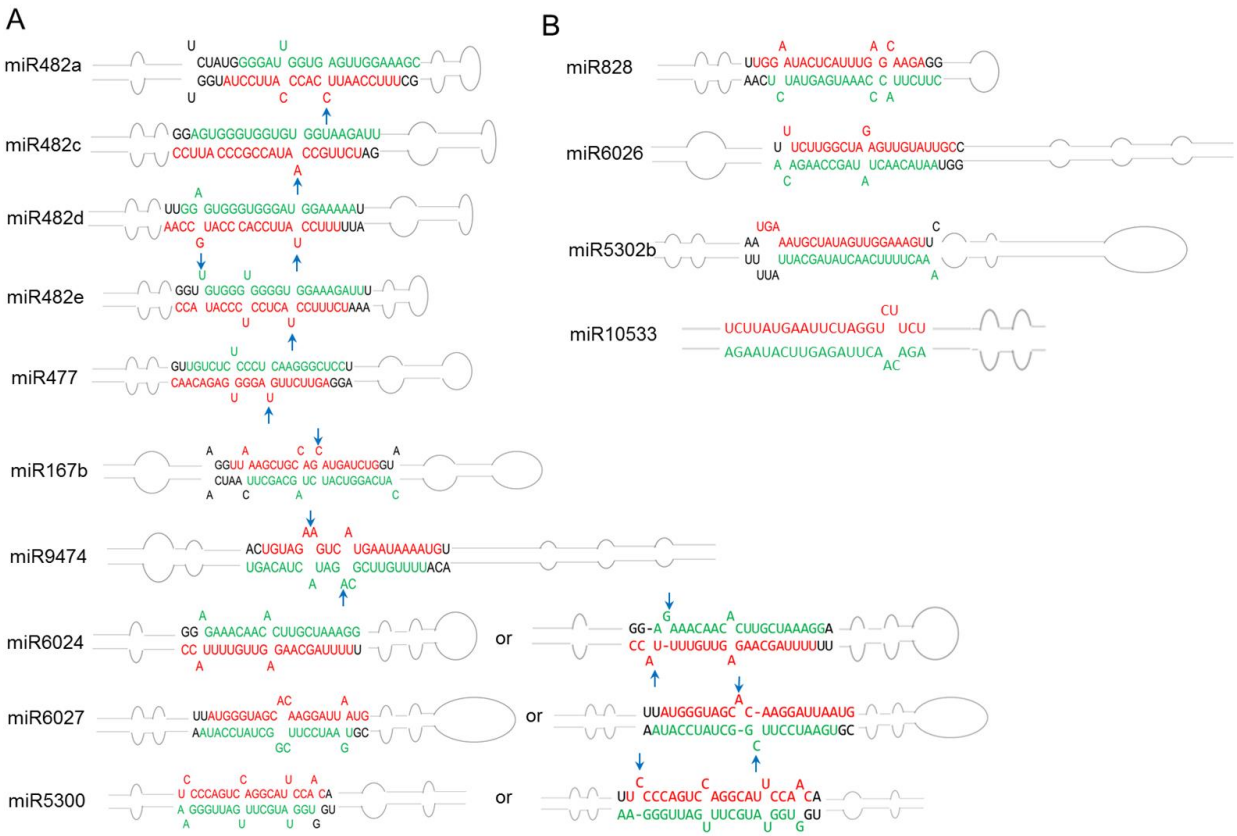

Supplemental Figure S13. miRNA foldback structures of slDCL1-dependent 22-nt miRNAs (**A**) and slDCL2-dependent 22-nt miRNAs (**B**). Arrows indicate the predicted asymmetric positions within the foldbacks.

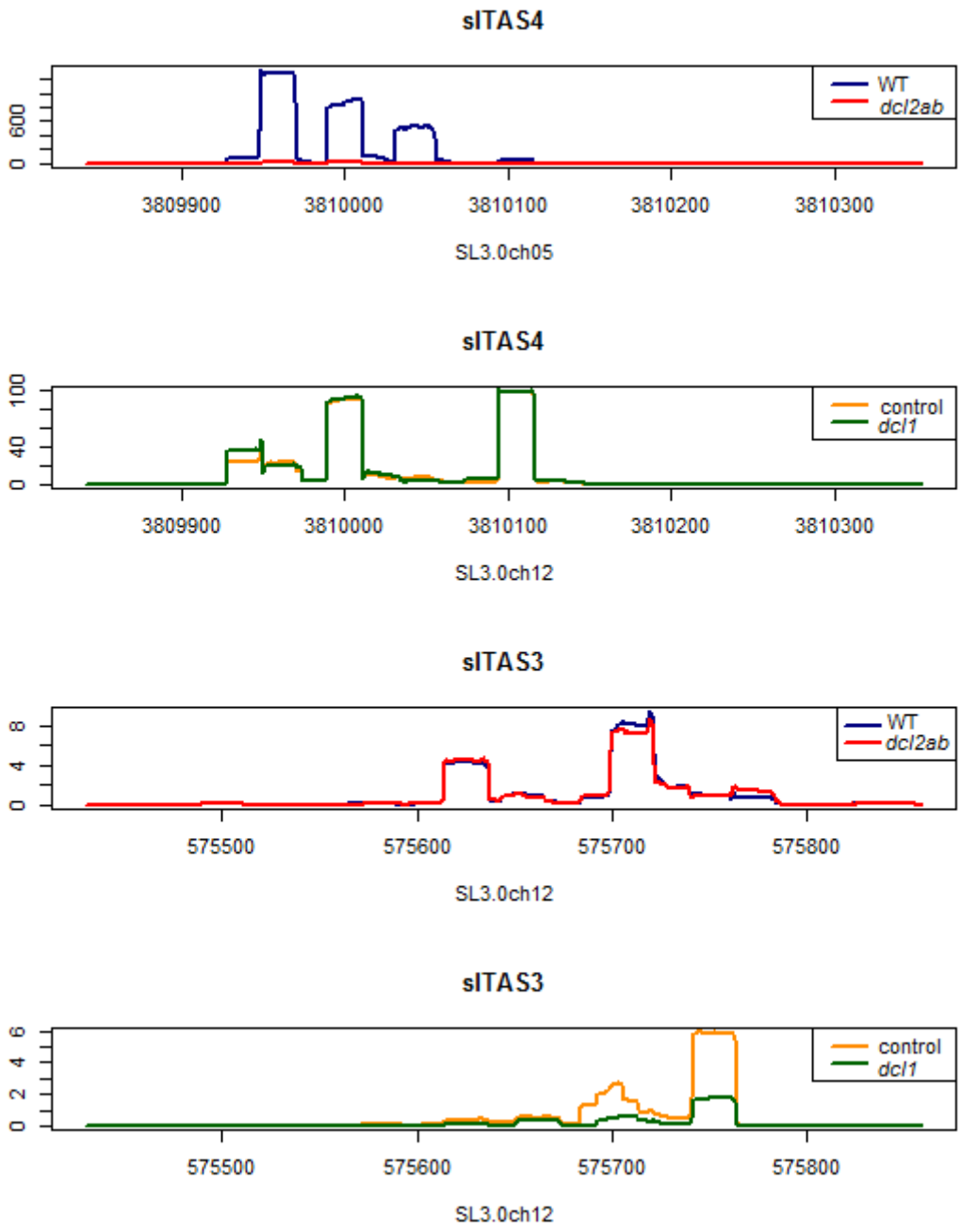

Supplemental Figure S14. The sRNA RPM plots showing the levels of tasiRNAs of slTAS4/slTAS3 in WT, *dcl1*, and *dcl2ab* For sRNA analysis in *dcl1*, as the *dcl1* samples differed drastically in miRNA from the control samples, we normalized sRNA to reads number of 24-nt sRNA in each sample, instead of reads number of total sRNA.

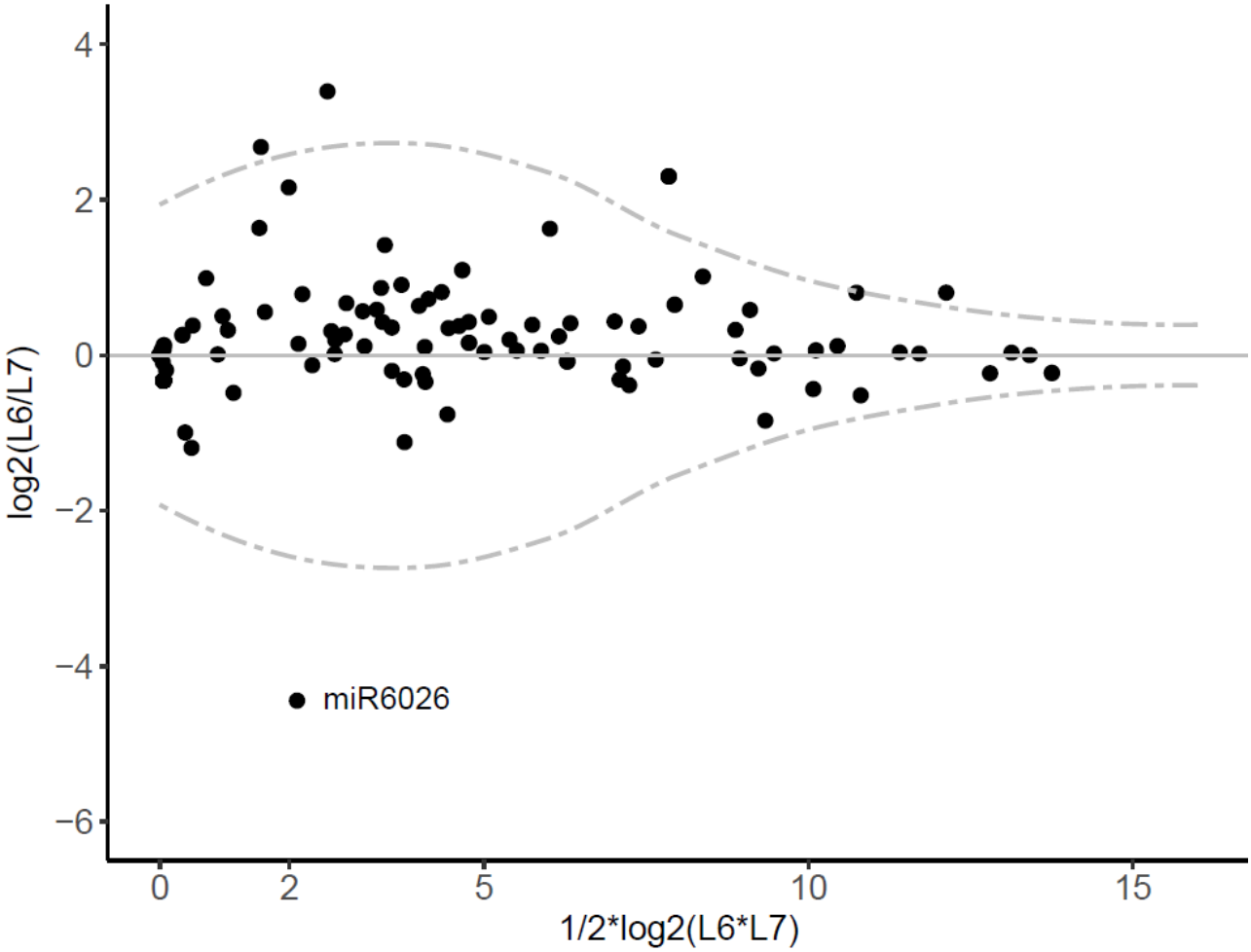

Supplemental Figure S15. MA Plot showing individual miRNA abundance levels in target mimic lines L7 (weak line) and L6 (strong line). Significantly differential expressed miRNAs ($p<0.05$) between L7 and L6 are marked.

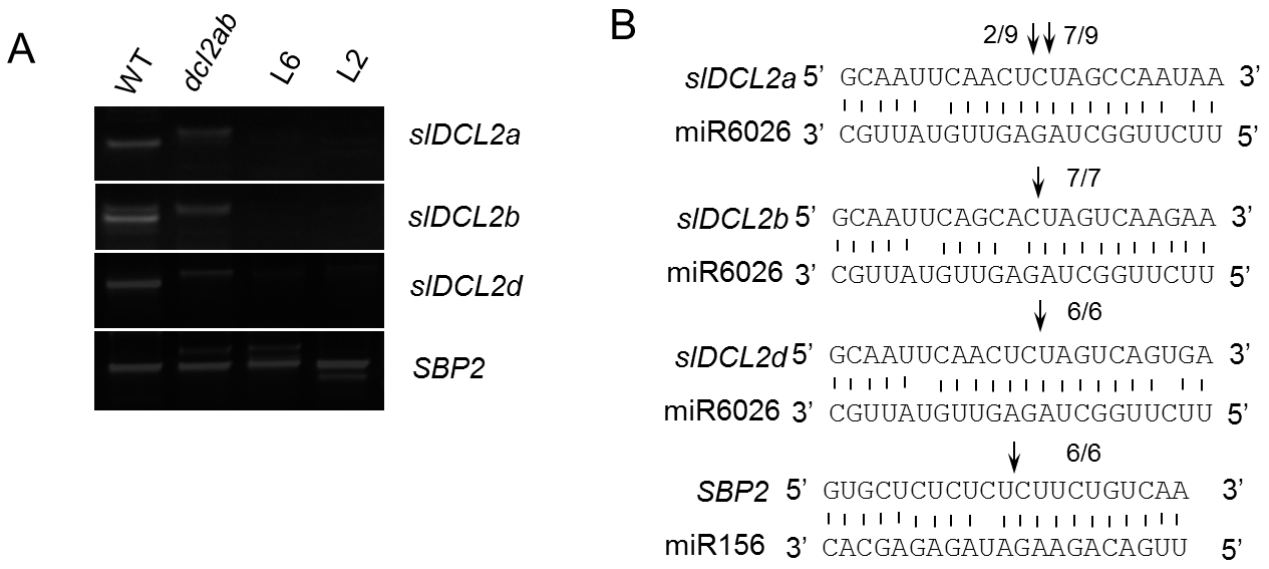

Supplemental Figure S16. Validation of miR6026-targeted *slDCL2* mRNA cleavage sites by 5'-RLM-RACE. **A.** RLM-RACE PCR results of 3' fragments of cleaved *slDCL2* mRNA from WT, *dcl2ab* and target mimic lines (L2 and L6), with *SBP2* as control; **B.** Sanger sequencing results of amplified products from WT showed in **A**. The arrows indicate the cleavage sites and the numbers show the frequency of clones sequenced.

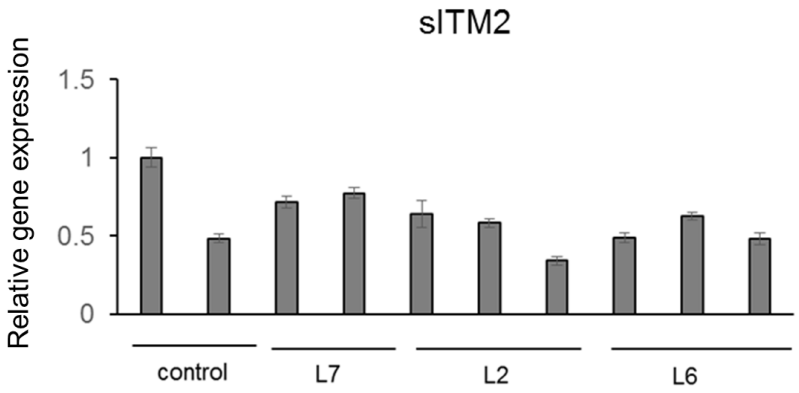

Supplemental Figure S17. Knock down of miR6026 does not affect the transcript level of *slTM2*. QRT-PCR of *slTM2* in control, weak mimicry line (L7), and strong mimicry lines (L2 and L6). *slActin7* was used as endogenous control.

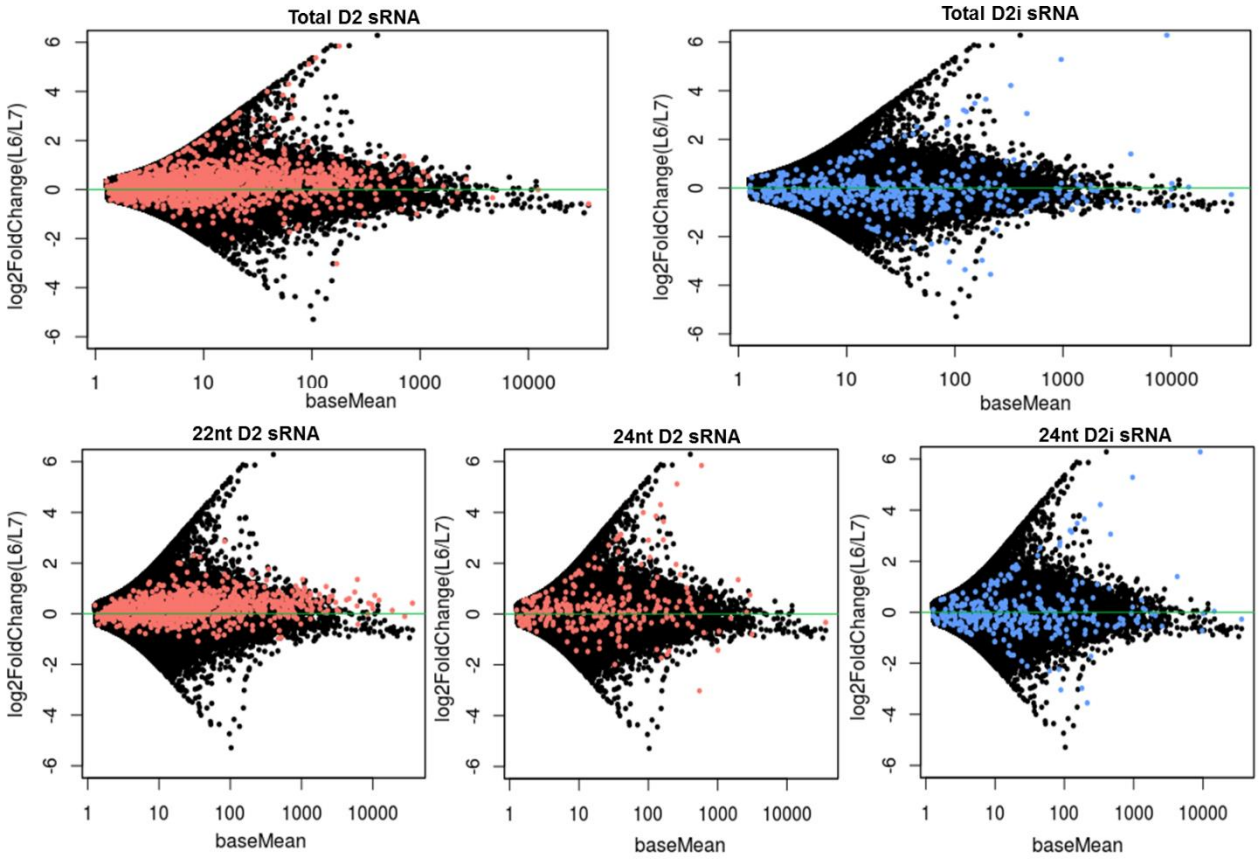

Supplemental Figure S18. MA plot showing accumulation of D2 and D2i sRNAs in L7 (weak mimic line) and L6 (strong mimic line). X axis represents the mean of normalized counts for each sRNA, whereas Y axis represents the log2 (RPM_L6/RPM_L7) of each sRN(A) D2 and D2i sRNAs are coloured in red and blue, respectively; Different sizes of D2 and D2i sRNAs are marked.

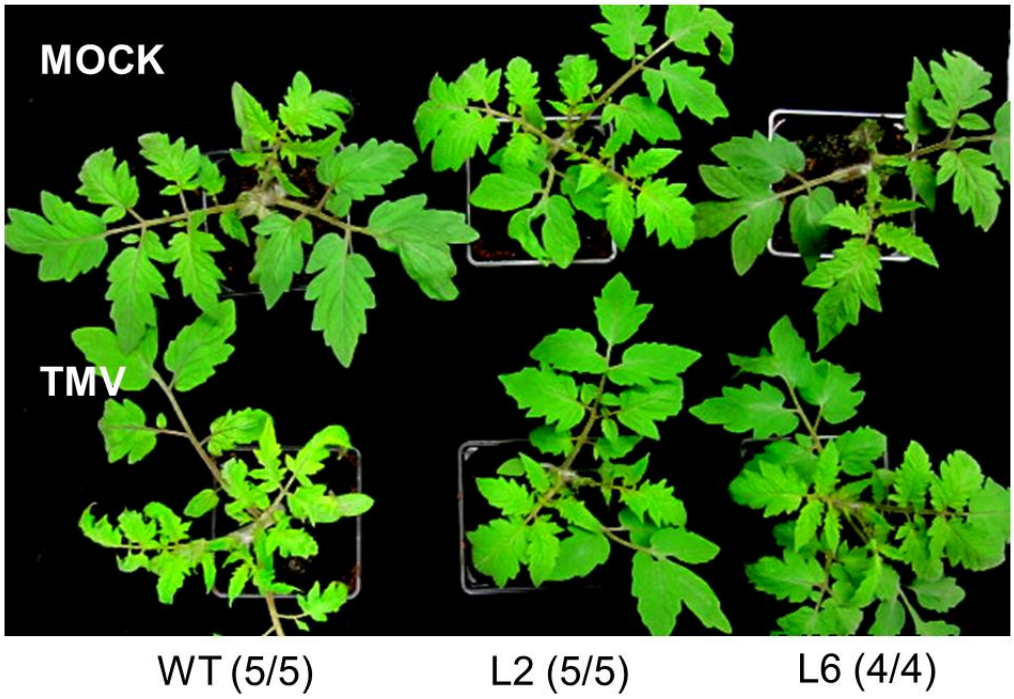

Supplemental Figure S19. Plants of two weeks after MOCK and TMV infection showing chlorosis and weaker chlorosis phenotypes of TMV infected WT and target mimic lines (L2 and L6), respectively; numbers in parenthesis show the number of plants with the representative symptoms and the number of infected plants

Supplemental Figure S20. Plants and leaves of 20 days (**A**) and 34 days (**B**) after TMV infection; Numbers in parenthesis show the number of plants with the representative symptoms and the number of infected plants. d. p. i., days post infiltration.

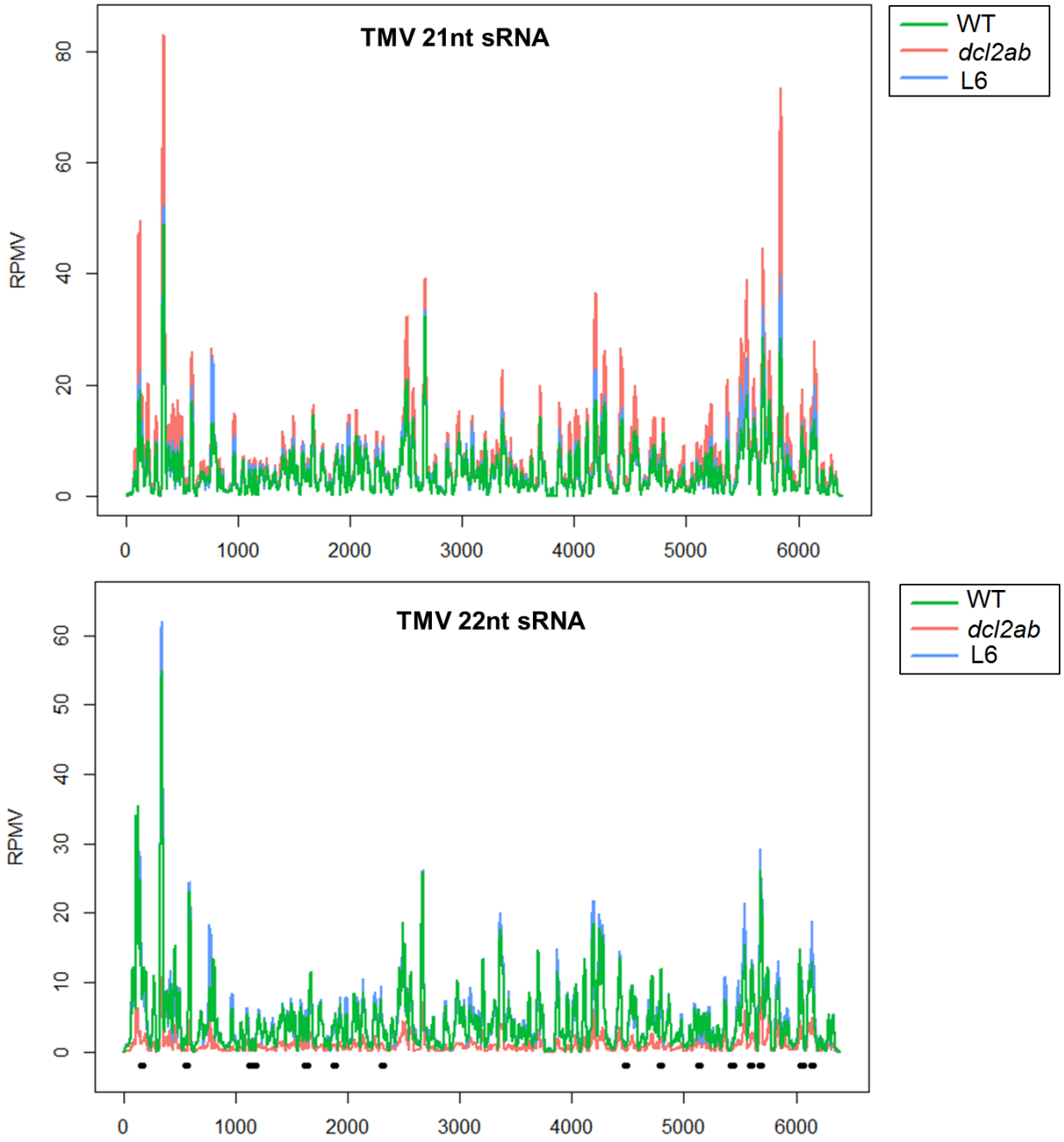

Supplemental Figure S21. The sRNA RPM plots showing the levels of TMV siRNAs in infected WT, dcl2ab and L6. The X axis indicates corresponding genome of TMV, the Y axis indicates the RPMV values (RPM normalized by TMV virus RNA amounts). Short bars under plots represent significantly ($p < 0.01$) upregulated 22nt sRNA in L6.

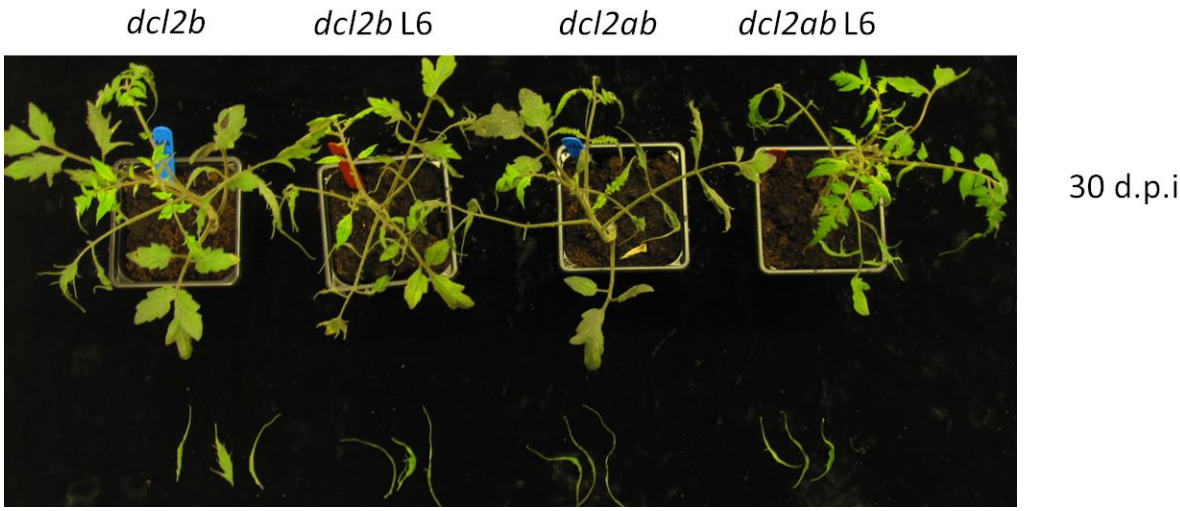

Supplemental Figure S22. Plants and leaves of 30 days after TMV infection. *dcl2b* L6 and *dcl2ab* L6 indicate *dcl2b* and *dcl2ab* plants with miR6026 target mimic through crossing with L6 respectively.

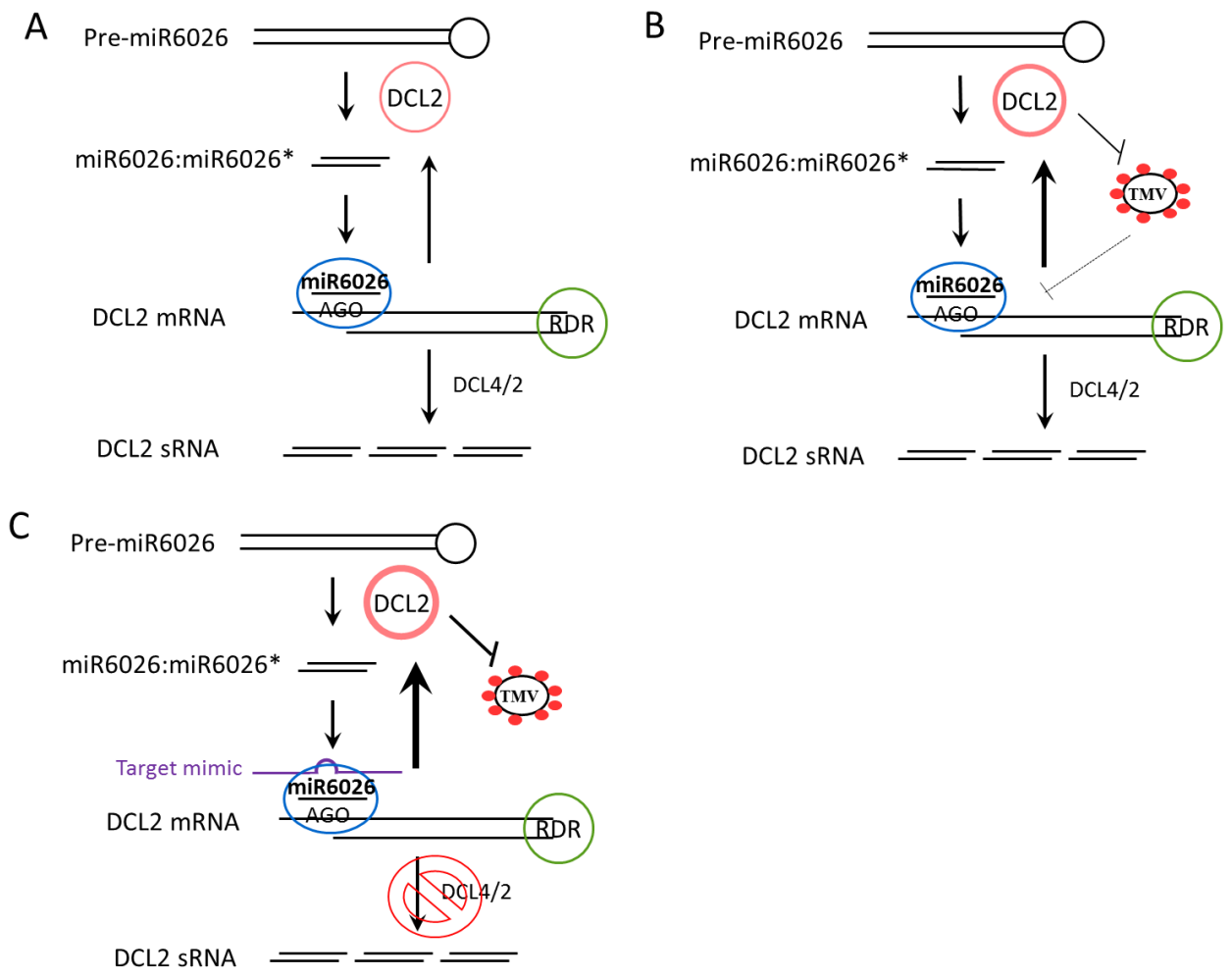

Supplemental Figure S23. Proposed working models. (**A**) Under normal condition, miR6026 is produced by SlDCL2 and targets SlDCL2 mRNA to generate secondary sRNA; (**B**) TMV infection upregulates SlDCL2b possibly through inhibiting miR6026-targeting of SlDCL2. Upregulate SlDCL2 contributes anti-viral function. (**C**) Target mimic eliminates miR6026 and thus prevents SlDCL2 from being targeted. Upregulate SlDCL2 elevates anti-viral activity.